Journal of Controlled Release

Research Article

Synergism between a Cell Penetrating Peptide and a pH-sensitive Cationic Lipid in Efficient Gene Delivery Based on Double-coated Nanoparticles

Ikramy A. Khalil[a,b,*] Seigo Kimura,[a] Yusuke Sato,[a] and Hideyoshi Harashima[a,*]

[a]*Faculty of Pharmaceutical Sciences, Hokkaido University, Kita-12, Nishi-6, Kita-ku, Sapporo 060-0812, Japan*

[b]*Faculty of Pharmacy, Assiut University, Assiut 71526, Egypt*

KEYWORDS: gene delivery, pDNA, YSK05, R8, nanoparticles

*Corresponding authors at: Laboratory for Molecular Design of Pharmaceutics, Faculty of Pharmaceutical Sciences, Hokkaido University, Kita-12, Nishi-6, Kita-ku, Sapporo 060-0812, Japan. Tel.: +81 11 706 3919. Email address: harasima@pharm.hokudai.ac.jp (H. Harashima) and ikramy@aun.edu.eg (I.A. Khalil)

ABSTRACT

We report on the development of a highly efficient gene delivery system based on synergism between octaarginine (R8), a representative cell penetrating peptide, and YSK05, a recently developed pH-sensitive cationic lipid. Attaching a high density of R8 on the surface of YSK05 nanoparticles (NPs) that contained encapsulated plasmid DNA resulted in the formation of positively charged NPs with improved transfection efficiency. To avoid the development of a net positive charge, we controlled the density and topology of the R8 peptide through the use of a two-step coating methodology, in which the inner lipid coat was modified with a low density of R8 which was then covered with an outer neutral YSK05 lipid layer. Although used in low amounts, the R8 peptide improved cellular uptake and endosomal escape of the DNA encapsulated in YSK05 NPs, which resulted in a high transfection efficiency. The two-step coating design was essential for achieving a high degree of transfection, as evidenced by the low activity of NPs modified with the same amount of R8 in a regular single-coated design. In addition, a high transfection efficiency was not observed when R8 or YSK05 were used alone, which confirms the existence of a synergistic effect between both components. The results of this study indicate that cationic cell penetrating peptides have the ability to improve transfection activities without imparting a net positive charge when used in the proper amount and in conjunction with the appropriate design. This is expected to significantly increase the potential applications of these peptides as tools for augmenting the activity of lipid nanoparticles used in gene delivery.

1. INTRODUCTION

Gene therapy is currently a subject of great interest since it represents one of the most promising medicines for treating diseases that are not currently treatable with conventional medicines [1–3]. Gene therapy relies on efficiently delivering a therapeutic nucleic acid such as plasmid DNA (pDNA) or small interfering RNA (siRNA) to an intracellular target site for the manipulation of gene expression for therapeutic purposes. The use of replication-defective viral vectors is currently the most efficient method for delivering nucleic acids to their intracellular target sites [4,5]. However, viral vectors suffer from several drawbacks including high immunogenicity, a high level of toxicity and difficulty of large-scale production. Synthetic non-viral vectors, i.e., liposomes, micelles, and dendrimers are promising alternates to viral vectors due to their simplicity, higher safety profiles and lower immunogenicity [6–9]. Non-viral vectors are recently applied for treating a wide-variety of acquired and inherited diseases including cancer, cystic fibrosis, cardiovascular and neurological diseases [10–16]. Despite the great progress that has been made in developing non-viral vectors in the past decade, the efficiency of such systems for use in gene therapy remains far below that of viral-based systems. Therefore, the greater challenge in non-viral gene delivery is developing systems that can overcome different extracellular and cellular barriers to efficiently and specifically deliver nucleic acids to their target sites in doses sufficient to produce a therapeutic effect [6].

Different strategies have been used for increasing the efficiency of non-viral systems including the use of novel polymers, peptides or lipids assembled in nano-delivery systems for protecting therapeutic nucleic acids and for improving their delivery to target sites inside cells [17–19]. A promising strategy depends on developing systems that combine two or more functional devices that have previously proven to be efficient and that function via different mechanisms. The

successful combination of such different functional devices in a single system is expected to increase the efficiency of gene delivery through synergistic effects of these devices. However, a rationalized design is required for controlling the topology of different components in a way that ensures that each one of them is functional at the right time and place.

We recently developed a pH-sensitive cationic lipid (referred to as YSK05) that is neutral at physiological pH but acquires a positive charge in acidic conditions [20]. YSK05 can condense and protect pDNA or siRNA by incorporating them into stable lipid nanoparticles (NPs) owing to its positive charge when used in an acidic medium [21–25]. Subsequent neutralization of the medium produces NPs with a neutral charge, which is advantageous for systemic administration where non-specific interactions and unwanted aggregation in the circulation can be avoided. In mice, YSK05 has been shown to mediate efficient pDNA delivery, resulting in efficient gene expression in hepatocytes after in vivo administration [25]. In addition, siRNA encapsulated in YSK05 NPs also resulted in efficient gene silencing in liver tissues in mice [23,24]. The efficiency of YSK NPs is related to its ability to adopt a positive charge in the acidic pH of endosomes, which may induce a structural change in the lipid membrane that facilitates its fusion with the endosomal membrane, thus allowing the internalized particles to escape efficiently from the endosomes [20]. It, therefore, appears that YSK05 is a promising functional device for developing efficient nucleic acid-based therapeutics. YSK NPs proved to be efficient despite the expected low cellular uptake and membrane interactions of YSK NPs after the loss of their positive charge. Therefore, it would be expected that the activity of YSK-based NPs could be further improved by using other functional devices that further enhance cellular uptake and interactions with membranes in general.

On the other hand, we have previously used the octaarginine peptide (R8) for efficient gene delivery in vitro and in vivo [26–31]. The positively charged R8 peptide was found to mediate efficient cellular uptake and improve the intracellular trafficking of its cargos, leading to an enhanced nuclear delivery of exogenous genes and improved gene expression [29,30]. Perhaps the most important disadvantage of the R8 peptide is its permanent positive charge, which limits its activity in vivo. Our extensive research with R8 led us to conclude that this peptide can still produce a dramatic improvement in gene delivery even when its positive charge is masked and not expressed on the surface.

In this study, we hypothesized that efficient gene delivery can be achieved through the use of a combination of YSK05 and R8 in a rationally designed system. We attempted to combine YSK05 and R8 in a synergistic non-positive design based on controlling the density and topology of the peptide. The simple mixing of YSK05 and low amounts of R8 resulted in the formation of a non-positive system, albeit with low transfection activity. To improve the activities, we examined the use of a two-step coating strategy for pDNA where only the inner lipid coat is modified with a low density of R8 while the outer lipid coat is mainly composed of YSK05 for achieving efficient endosomal escape. The proposed design proved to be essential for achieving a successful synergism between YSK05 and R8. We further identified the mechanism responsible for this synergism, which indicated that the cationic R8 peptide has the ability to play multiple roles in gene delivery that extend far beyond simply the introduction of a positive charge to the system.

2. MATERIALS AND METHODS

2.1. Materials

HeLa human cervix carcinoma cells were obtained from the RIKEN Cell Bank (Japan). Dioleoylphosphatidylethanolamine (DOPE) and cholesterol (chol) were purchased from Avanti Polar Lipids (Alabaster, AL). 1,2-Dimyristoyl-sn-glycerol, methoxypolyethylene Glycol 2000 (DMG-PEG) was purchased from the NOF CORPORATION (Tokyo, Japan). Stearyl-octaarginine (STR-R8) was purchased from Toray Research Center, Inc. (Tokyo-Japan). Chloroquine was purchased from WAKO Pure Chemicals (Osaka, Japan). The reporter plasmid pcDNA3.1(+)-luc (7037 bp) encoding the firefly luciferase gene was purified using a Qiagen Endofree Plasmid Mega Kit (Qiagen GmbH, Helden, Germany). Dulbecco`s modified eagle medium (DMEM) and fetal bovine serum (FBS) were purchased from Invitrogen Corp. (Carlsbad, CA, USA). The luciferase assay reagent and reporter lysis buffer were obtained from Promega Co. (Madison, USA). All other reagents were reagent-grade and commercially available.

2.2. Preparation of conventional 1-step coated NPs

Nanoparticles were prepared by the lipid hydration method, as previously described [32]. The lipids were mainly composed of YSK05:DOPE:Chol:DMG-PEG (4:4:2:0.15). The lipids (320 nmol) were dissolved in ethanol (300 µl) in a round bottom glass tube and the ethanol was then removed by evaporation by a stream of Nitrogen. The pDNA (15 µg) was diluted in 500 µl HEPES buffer (10 mM, pH = 4) and the solution was used to hydrate the lipid film for ~15 min at room temperature. The tubes were then sonicated in a bath type sonicator and incubated at room temperature for 30 min. The medium in the final solution was adjusted to pH 7.4.

2.3. Preparation of 2-step coated NPs

The lipids used in the first coat (DOPE/STR-R8; total 160 nmol) were dissolved in ethanol and evaporated to form a lipid film (tube 1). The lipids used in the second coat (YSK05/chol/DMG-PEG; total 160 nmol) were dissolved in ethanol and evaporated to form a second lipid film (tube 2). The pDNA (15 µg) was dissolved in 500 µl HEPES buffer (10 mM, pH = 4) and the solution was used to hydrate the lipid film in tube 1 for 15 min at room temperature. The tube was sonicated in a bath type sonicator and incubated for 30 min at room temperature. The contents were then transferred to tube 2 and incubated with the second lipid film for 15 min. The second tube was then sonicated for ~1 min and incubated for 30 min at room temperature and the pH was adjusted to 7.4. NPs were characterized by measuring the diameter and surface charge using Zeta-sizer Nano ZS ZEN3600 instrument (Malvern, UK). A Picogreen assay kit (Molecular Probes, Eugene, USA) was used to determine the final pDNA concentration and the encapsulation efficiency according to the manufacturer's protocol.

2.4. Transfection studies

HeLa cells were cultured in DMEM supplemented with 10% heat-inactivated fetal bovine serum (FBS), penicillin (100 U/mL) and streptomycin (100 µg/mL) at 37^{o}C in an atmosphere of 5% CO_2 and 95% humidity. One day before transfection, cells were cultured in a 24-well plate (40,000 cells per well). At the time of transfection, the culture medium was removed and cells were washed with 500 µL of DMEM without serum. Samples containing 0.4 µg pDNA suspended in 250 µL DMEM were added to each well and cells were incubated for 1 hr at 37^{o}C. Fresh DMEM (1 mL) containing 10% FBS was then added followed by further incubation for 23 hr. At the end of the incubation, the medium was removed and cells were washed with phosphate buffered saline (PBS) 500 µL then solubilized by the addition of 75 µL Reporter Lysis Buffer

(Promega). Luciferase activity in the cell lysate was measured in the presence of a Luciferase Assay Reagent (Promega) by means of a luminometer (Luminescence-PSN, ATTO, Japan). The amount of total proteins in the cell lysates was measured using a BCA protein assay kit (Pierce, Rockford, IL, USA). Each transfection experiment is performed in triplicate. To examine the effect of chloroquine, cells were incubated with DMEM containing chloroquine (final concentration 100 μM) for 4 hours. The medium was then removed and cells were washed and incubated with DMEM containing the various MENDs and chloroquine for 1 hr. The medium was then replaced with 1 mL of fresh medium containing serum and the incubation continued for 23 hr.

2.5. Flow cytometer studies

One day before the experiments, HeLa cells were cultured in a 6-well plate (200,000 cells per well). The different NPs were prepared as described above where a DiD label (Invitrogen, CA, USA) was mixed with the lipids (0.5 mol% of total lipids). At the time of the experiments, the culture medium was removed and cells were washed with 1 mL DMEM without serum. Samples containing pDNA suspended in 1 mL DMEM was added to each well and the cells were incubated for 1 hr at 37^{o}C. The medium was then removed and cells were washed 3 times with phosphate buffer saline and then trypsinized. The cell suspension was centrifuged (700 g, 4^{o}C, 3 min) and the precipitated cells were suspended in 1 mL FACS buffer (PBS containing 0.5% bovine serum albumin and 2mM EDTA). Centrifugation and re-suspension in FACS buffer were repeated twice before the final cell suspension was passed through a nylon mesh to remove any cell aggregates. The fluorescence of the cells was analyzed by means of a FACS Calibur flow cytometer (FACScan, Becton Dickenson).

2.6. Confocal microscopy studies

One day before the experiment, HeLa cells were cultured on a 35-mm glass base dish (100,000 cells per dish). pDNA was labeled with Cy5 using a Label IT Cy5 labeling kit (Mirus Corp., Madison, US) following the manufacturer's protocol. At the time of the experiments, the culture medium was removed and cells were washed with 1 mL DMEM without serum. Samples containing Cy-5 labeled pDNA suspended in 1 mL DMEM was added to each well and cells were incubated for 1 hr at 37^{o}C. The medium was then removed and cells were incubated in DMEM medium with 10% serum for a 3-hr chase period. LysoTracker Green (Molecular Probes, Eugene, OR) was added to the medium (1 μM) 30 min before examination with confocal microscopy (Olympus).

2.7. Statistical analysis

Comparisons between multiple treatments were made utilizing the one-way analysis of variance (ANOVA) followed by Bonferroni or Student-Newman-Keuls test. Pair-wise comparisons between treatments were made using a two-tail Student t-test. A p-value of <0.05 was considered to be significant.

3. RESULTS

3.1. Modification of YSK05 nanoparticles with R8

We condensed luciferase-encoding pDNA into YSK05 NPs in the presence and absence of R8. A solution of the pDNA in an acidic medium was added to a lipid film consisting mainly of the pH-sensitive YSK05 and the helper lipid DOPE with or without STR-R8. The peptide was used in two different amounts: low (YSK/R8-L; 2 mol% of the total lipids) and high (YSK/R8-H; 10 mol% of the total lipids). The amount of R8 added was selected based on preliminary data from experiments in which negative or positive NPs (YSK/R8-L or YSK/R8-H, respectively) were prepared (data not shown). The diameters and charges of the different NPs are shown in Table 1. All NPs showed diameters ranging from 170 to 190 nm. Nanoparticles containing high amount of R8 were positively charged while those prepared with low R8 amounts or lacking R8 were negatively charged. The transfection activities for the different NPs are shown in Figure 1. The activity of the YSK NPs was increased by ~8-fold by the addition of low amounts of R8 and ~107-fold by the addition of high amounts of R8. This result indicates that R8 modification can improve the transfection activities of YSK NPs depending on the dose of R8 used and the net surface charge of the NPs. Although YSK and YSK/R8-L NPs were found to have similar diameters and surface charges, the activity of the latter was higher, indicating that R8 may play a role in gene delivery, even when the amount is low and the system is not carrying a net positive charge.

TABLE 1. Characterization of YSK nanoparticles*

	STR-R8 content (mol% of total lipids)	Diameter (nm)	PDI	Zeta Potential (mV)
YSK	0	181.5 ± 11.7	0.38 ± 0.06	(-) 20.2 ± 6.8
YSK/R8-L	2	181.4 ± 10.7	0.31 ± 0.06	(-) 19.5 ± 5.8
YSK/R8-H	10	178.1 ± 6.3	0.35 ± 0.13	(+) 22.5 ± 7.5

*Values are the mean +/- SD of at least 3 independent preparations

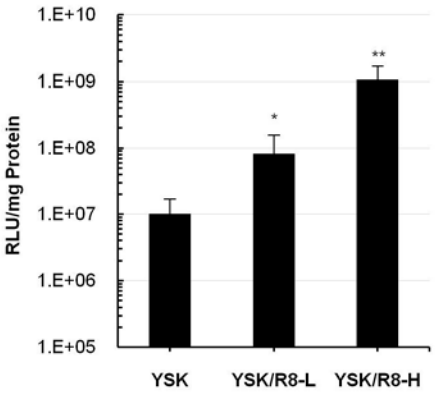

Figure 1. Comparison of transfection activities of luciferase-encoding plasmid DNA encapsulated in different YSK NPs.

3.2. Preparation and evaluation of double coated YSK/R8 nanoparticles

Although R8 used in low amounts improved the activity of YSK-NPs as shown in Figure 1, we hypothesized that the activity of YSK/R8-L could be further optimized by controlling the position of the R8 peptide and the YSK05 lipid. We proposed a new strategy for preparing such devices, based on two-step coating (Figure 2A). In this design, a lipid film consisting of DOPE and a low amount of R8 is used to condense pDNA into negatively charged NPs. The resulting NPs are then further coated with an outer coat consisting mainly of YSK05 through electrostatic attractions between the negatively charged NPs and the positively charged YSK05 in an acidic

medium. Thus, the R8 peptide is presumably masked and located within the inner coat. To prepare the first coated NPs, pDNA was condensed with a lipid consisting of DOPE and increasing amounts of STR-R8 (3 to 8 mol% of lipid). As shown in Figure 2B, increasing the amount of R8 changed the surface charge from negative to positive. Since the objective was to prepare negative NPs to be further coated with a second coat, only NPs containing 4, 5, or 6 mol% of lipid were further coated with a second coat of YSK and cholesterol. Positively charged NPs containing 7 or 8 mol% lipid would not be expected to accept a second coat since both have similar positive charges. The outer lipid included a low amount of DMG-PEG (3% of the outer lipid) to control particle diameter and prevent the near neutral NPs from forming aggregates. The properties of the NPs after a second coating are shown in Figure 2C. The diameter was around 140 to 160 nm and the charge changed from negative to neutral or slightly positive when the amount of R8 was increased. The encapsulation efficiency (EE) of the NPs after the first coat was low (20-32%) since the amount of R8 is not sufficient to fully condense the DNA (Figure 2D). However, the EE was increased by the second coating especially when the inner lipids contained 4 mol% of R8. This can be explained by the fact that the first coat is more negative when 4 mol% of R8 is used compared to 5 or 6 mol%, and NPs with a more negative charge would be expected to be more extensively covered by the second positively charged lipid coat. This demonstrates the clear advantage of a second coat in enhancing the EE of the pDNA in the lipid NPs. We next examined the transfection activities of different NPs after the first or second coating (Figure 2E). After the first coating, the NPs containing a lower amount of R8 (4 mol%) showed the highest activity. When R8 approaching a neutral charge was used (5 or 6 mol%), some aggregation was detected, as evidenced by their larger diameters (data not shown), which may explain the lower activities of these NPs. However, the second coat significantly increased

transfection activities by 6-fold (4 mol%), 60-fold (5 mol%), or 126-fold (6 mol%). This improvement can be explained by the endosomal escape ability of the YSK05 located in the outer coat as well as the improved EE after the second coating [20,22]. The higher improvement in the case where 5 or 6 mol% of R8 was used can be explained by a change in the charge of NPs to less negative and loss of aggregation due to the presence of PEG in the outer coat. The transfection activities after the second coat were remarkably high and compete with Lipofectamine 2000 reagent (LF), one of the most efficient commercially available transfection systems, although the NPs are not carrying a net positive charge in all three cases (Supplementary Figure S2). This result indicates the importance of controlling the position of the peptide (inner or outer) and clearly shows a possible advantage of the double-coating strategy compared to conventional single-coating strategy shown in Figure 1.

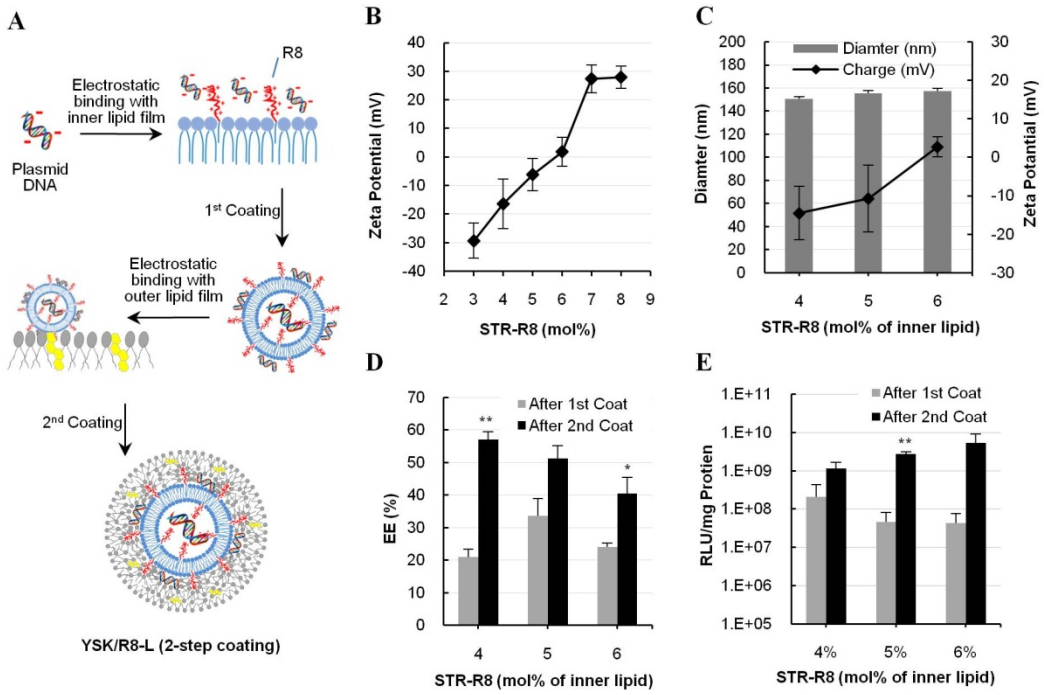

Figure 2. Preparation and evaluation of double-coated YSK/R8 NPs

3.3. Optimization of double coated YSK/R8-L nanoparticles

Since the objective was to develop non-positively charged NPs to avoid non-specific interactions, we avoided using 5 or 6 mol% of R8 in the inner lipid. We fixed the amount of R8 at 4.5 mol% of the inner lipid, since this condition showed a high transfection activity and resulted in all preparations having a final negative charge. However, the EE was still low (~40-50%) which may represent a significant barrier for in vivo applications. We increased the total amount of lipid from 320 to 800 nmol while fixing the ratio of inner to outer lipid (1:1) and fixing the amount of R8 in the inner lipid (7.2 nmol/15 µg pDNA). We then characterized the preparations and measured the luciferase activities of the different NPs (Figure 3). Increasing the amount of total lipids decreased the negative charge but had negligible effects on particle diameter. The EE increased from ~40 to ~80% by increasing the amount of lipid, while the transfection activity increased up to total lipid 640 nmol. Cytotoxicity started to significantly increase when the total amount of lipid was higher than 640 nmol as judged by measuring total protein content at the end of the transfection period (data not shown), which may explain the decreased activity for NPs prepared using 800 nmol of lipid. Changing the amount of YSK or the ratio of inner to outer lipids did not further improve EE or luciferase activity (data not shown). Therefore, YSK/R8-L NPs prepared with 640 nmol lipids were used in further studies.

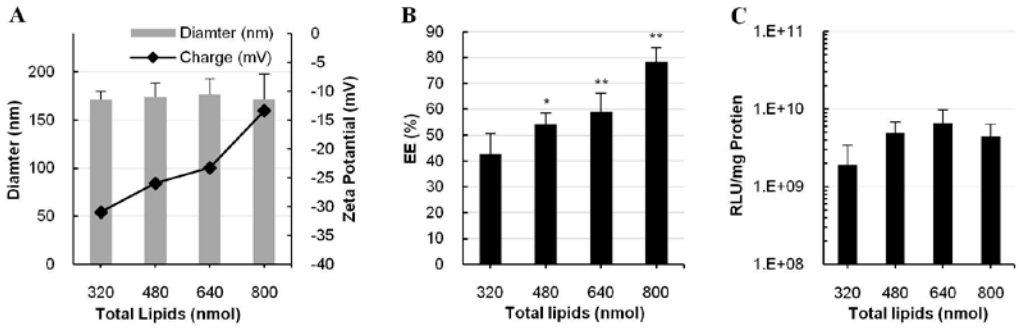

Figure 3. Optimization of double-coated YSK/R8 NPs

3.4. Comparing NPs prepared with 1-step or 2-step coating

We next directly compared the luciferase activity of YSK/R8-L and YSK/R8-H NPs prepared with the ordinary 1-step coating or with the proposed 2-step coating. The same amount of lipid and composition were used when comparing 1-step versus 2-step coating so that the only difference was in the method used in the preparation, which determines the position of the peptide. In the case of YSK/R8-L, R8 is located at the outer surface (1-step coating) or in the inner lipid coat (2-step coating). In the case of YSK/R8-H, R8 is located at the outer surface (1-step coating) or both in the inner lipid and outer surface (2-step coating). The inner lipid coat was the same for R-L and R-H NPs. When a high amount of R8 was attached to the inner coat only, positive NPs were produced that could not been further coated with a positively charged YSK05 second coat due to lack of electrostatic attraction. The lipid composition and characterization of the different NPs are shown in Table 2. YSK/R8-L NPs were negative while YSK/R8-H NPs were positive. As shown in Figure 4A, the YSK/R8-L prepared with 2-step coating produces a dramatically higher transfection activity compared to the 1-step coating (~70-fold increase). This clearly shows the advantage of a 2-step coating (or positioning R8 in the inner coat) in the case where low amounts of R8 were used. Meanwhile, there was no significant difference between NPs prepared with the 1-step or 2-step coating in the case of YSK/R8-H, probably because a high amount of R8 is located at the outer surface in both cases. Noticeably, the activity of the YSK/R8-L (2-step) NPs was comparable to that of YSK/R8-H. The transfection activities of optimized YSK/R8-L and YSK-R8-H was less than LF but the difference was not statistically significant (Supplementary Figure S2B). Although the exact mechanism responsible for this high activity of YSK/R8-L (2-step) NPs was not evident at this stage, the results confirmed the importance of controlling the position of the peptide (inner or outer), which is dependent on the

amount of peptide used. We additionally examined the transfection activities of YSK/R8-L and YSK/R8-H in the absence or the presence of 10% serum to investigate the potential applicability of the NPs for in vivo gene delivery (Figure 4B). The presence of serum reduced the transfection activities by ~30% in the case of R8-L compared to ~70% in the case of R8-H. This shows that non-positive YSK/R8-L is relatively more serum resistant compared to positively charged systems such as YSK/R8-H.

TABLE 2.

Composition and characterization of different nanoparticles prepared by 1-step or 2-step coating*

		Lipid Composition	Diameter (nm)	PDI	Zeta Potential (mV)
YSK/R8-L	1-step coating	YSK:DOPE:Chol:PEG:R8[1] (4:5:1:0.075:0.1125)	168 ± 1	0.270 ± 0.00	(-) 24 ± 7
	2-step coating	*First Coat*- DOPE:R8 (9.775:0.225) *Second Coat*- YSK:Chol:PEG (8:2:0.15)	162 ± 3	0.282 ± 0.02	(-) 27 ± 2
YSK/R8-H	1-step coating	YSK:DOPE:Chol:PEG:R8 (4:5:1:0.075:0.6125)	140 ± 4	0.242 ± 0.07	(+) 34 ± 7
	2-step coating	*First Coat*- DOPE:R8 (9.775:0.225) *Second Coat*- YSK:Chol:PEG:R8 (8:2:0.15:1)	144 ± 1	0.265 ± 0.02	(+) 25 ± 7

*Values are the mean +/- SD of at least 3 different preparations
[1]PEG is used as DMG-PEG-2000 and R8 is used as STR-R8

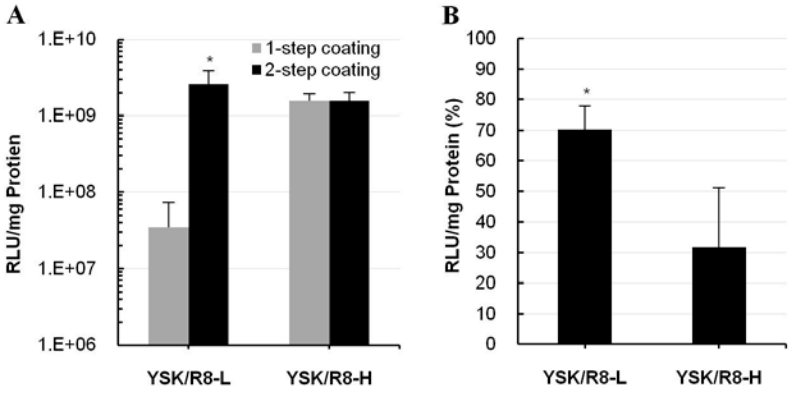

Figure 4. Comparison of transfection activities of different NPs prepared with 1-step or 2-step coating

3.5. Synergism between YSK05 and R8

To investigate the synergistic effect of the use of a combination of YSK05 and R8, we compared the transfection activities of NPs prepared with YSK05/DOPE (without R8) with those prepared with DOPE/STR-R8 (DOPE/R8-L and DOPE/R8-H, both without YSK) or those prepared with both YSK05 and R8 (YSK/R8-L and YSK/R8-H) (Figure 5). NPs prepared without R8 (YSK) showed relatively low transfection activities. The use of low amounts of R8 without YSK05 (DOPE/R8-L) did not significantly increase the activity. However, the activity significantly increased when YSK05 was combined with a low amount of R8 (YSK/R8-L) particularly in the 2-step design. This indicates the existence of a synergistic effect of YSK and R8 and validates our hypothesis that there are distinct advantages of combining these two different functional devices in a single system. A similar synergism was shown when high amounts of R8 were used (Figure 5B). However, the activity of DOPE/R8-H was relatively higher than similar NPs prepared with a low amount of R8 (DOPE/R8-L). This is consistent with our previous results showing that high amounts of R8 are needed to improve the intracellular trafficking of liposomes and NPs when YSK05 is not used [30]. Hence, the synergistic effect of YSK05 and R8 is particularly evident when preparing non-positive NPs using low amounts of R8; a condition that is highly desirable for in vivo application.

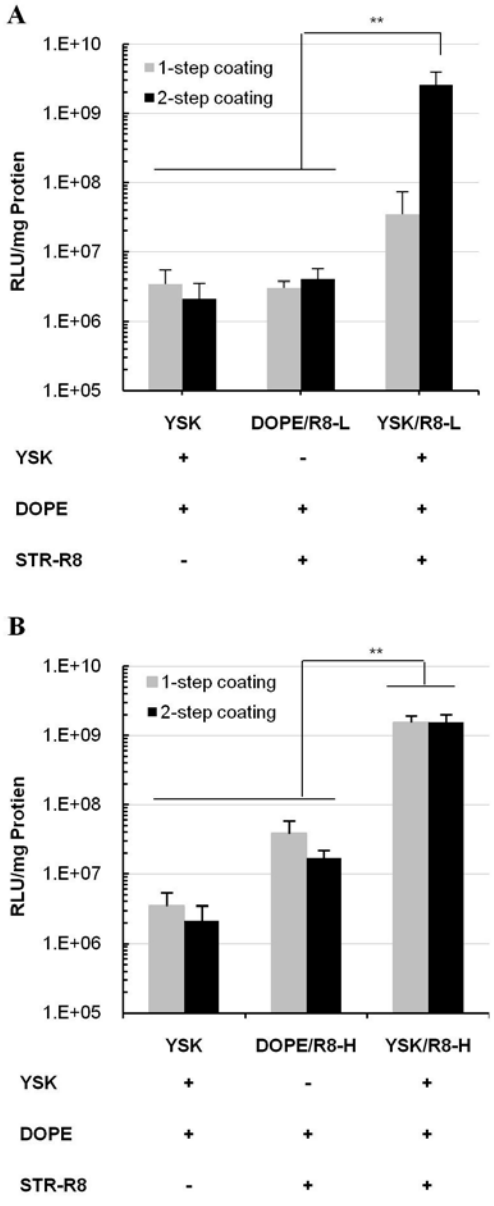

Figure 5. Synergism between YSK and R8

3.6. Cellular uptake of different nanoparticles

To understand the mechanism of synergism between YSK05 and R8, we examined the cellular uptake of different double-coated NPs prepared with DiD-labeled lipids using flow cytometry. The uptake of NPs was low in the absence of R8 (YSK) and was only slightly increased when YSK05 was replaced with DOPE and low amounts of R8 (DOPE/R8-L) (Figure 6, A-B). However, the uptake was significantly improved by ~6-fold when YSK05 was combined with a low amount of R8 (YSK/R8-L). Nevertheless, the improvement in uptake cannot explain the large difference in transfection activities of YSK and YSK/R8-L NPs (~700 fold). This shows that the role of R8 in improving intracellular trafficking of YSK NPs is probably more important than its role in enhancing cellular uptake. In the case where a high amount of R8 was used (Figure 6, C-D), the presence of R8 caused a high cellular uptake (~10-12 fold increase). In this case, the high R8 density on the surface was sufficient to cause a high cellular uptake, even in the absence of YSK05 (DOPE/R8-H). To further examine the intrinsic efficiency of each type, we divided the transfection activities (RLU/mg of protein) by the amount internalized (geo-mean fluorescence) in each case (Figure 6, E). The efficiency was relatively low when either YSK or R8 were used alone. The efficiency was higher when YSK was combined with R8, which confirms the role of R8 in improving intracellular trafficking when used in low amounts (inner) or high amounts (inner and outer). Although the highest uptake was shown in the case of DOPE/R8-H, the efficiency of these YSK-lacking NPs was low, which clearly points to the importance of using YSK for enhancing endosomal escape.

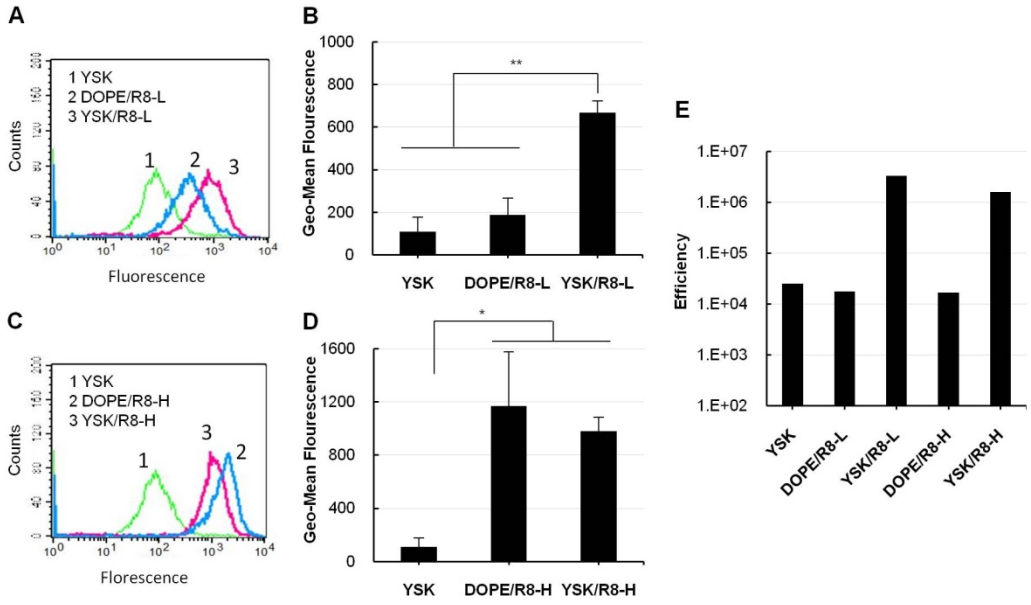

Figure 6. Comparison of cellular uptake and transfection efficiency of NPs

3.7. Endosomal escape of different nanoparticles

Since the difference in cellular uptake did not explain the difference in transfection activities of YSK and YSK/R8-L NPs, we examined the endosomal escape of both types prepared using Cy-5-labeled pDNA. We observed cells incubated with YSK or YSK/R8-L NPs using confocal scanning microscopy where the lysosomes were stained with LysoTracker. Representative images of observed cells are shown in Figure 7. The amount internalized appeared to be higher in the case of YSK/R8-L, which is consistent with the flow cytometer data shown in Figure 6. Furthermore, the pattern of co-localization between pDNA and lysosomes is different. A higher co-localization (yellow spots) was more evident in the case of YSK NPs. In the case of YSK/R8-L NPs, a high amount of pDNA was not localized with lysosomes, which indicates that the pDNA is not highly entrapped in the endosomal/lysosomal compartment. This result shows that

R8 has the ability to enhance YSK-mediated endosomal escape. We assume that R8 may enhance the interaction between YSK and endosomal membranes, thus leading to a more efficient disruption of endosomes and the release of pDNA to the cytosol. To further confirm this result, we measured transfection activities in the absence and presence of the endosome-disrupting agent, chloroquine (Figure 8) [33]. The disruption of endosomes by chloroquine enhanced the transfection activities in the case of YSK NPs by ~2-fold, indicating that a significant amount of pDNA was trapped in the endosome/lysosome compartment. Meanwhile, transfection activities were not significantly increased by chloroquine in the case of YSK/R8-L, indicating that endosomal escape is already efficient in this case. This is consistent with the previous confocal microscopy study, which showed an efficient endosomal escape when a combination of YSK and R8 was used. Collectively, these results confirm that R8 has the ability to improve cellular uptake as well as the endosomal escape of the YSK05-NPs.

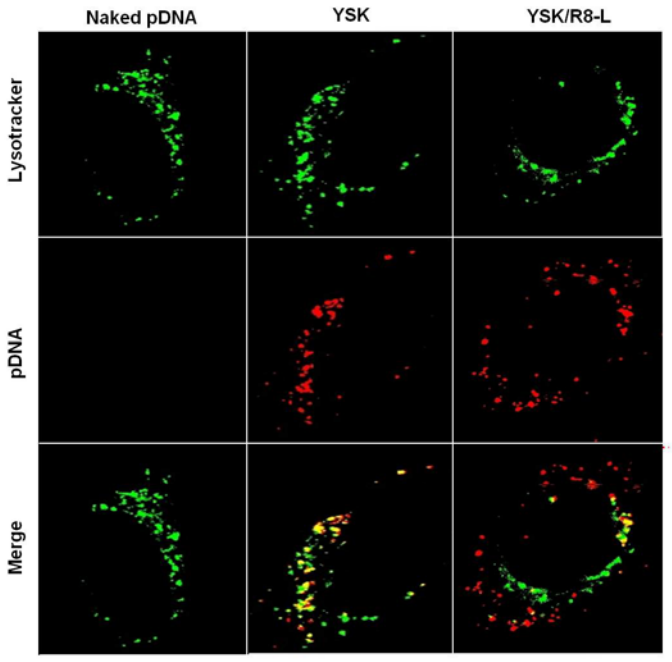

Figure 7. Evaluation of endosomal escape of different NPs

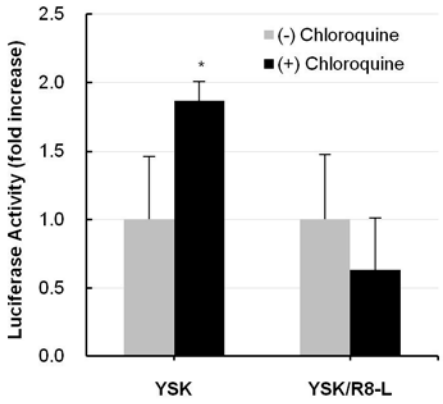

Figure 8. Effect of chloroquine on transfection activities of different NPs

4. DISCUSSION

YSK05, a pH-sensitive cationic lipid, efficiently delivered pDNA and siRNA to the cytosol of liver cells after systemic administration [20-25]. This lipid contains a pH-sensitive group (N-methylpiperidine) and two unsaturated carbon chains. At acidic pH, it becomes positively charged (pKa = 6.6) and can be used to condense a variety of different nucleic acids. Upon changing the pH to neutral, YSK05 nanoparticles lose their positive charge and can be internalized into cells through Apo-E mediated endocytosis [34]. After internalization into endosomes, the YSK lipid causes efficient endosomal escape since it adopts an inverted hexagonal shape with anionic lipids when the pH drops below 6. Compared with NPs prepared using conventional cationic lipids, fewer YSK-NPs are internalized into cells, but they produce a stronger gene silencing activity [20]. The low internalization of YSK NPs can be explained by the fact that these NPs are neutral under physiologic pH, which limits their internalization compared to systems prepared with cationic lipids. Therefore, the addition of a ligand that can enhance the cellular uptake of YSK NPs would be expected to increase the number of particles that are internalized and subsequently improve transfection activities.

The R8 peptide is a model CPP peptide that enhances cellular uptake and controls the intracellular trafficking of its attached cargos [29,30]. We hypothesize that a combination of R8 and YSK may cause high transfection activities, since R8 can enhance the interactions between the lipids contained in NPs and cellular or endosomal membranes. When R8 was attached on the surface of YSK NPs prepared with luciferase-encoding pDNA, the transfection activities were increased based on the density of the peptide used (Figure 1). Using a low R8 density resulted in the formation of negatively charged NPs whose activities were ~8 fold higher than NPs prepared without R8. The use of a high R8 density produced positively charged NPs whose activities were

~107 fold higher than NPs prepared without R8. We suggest that R8 may improve the interactions between YSK and cellular or endosomal membranes leading to increased cellular uptake or endosomal escape, respectively. R8 actually improved the cellular uptake of YSK NPs when used in low or high density (Figure 6). In addition, R8 also improved the endosomal escape of YSK NPs as evidenced by confocal microscopy results (Figure 7).

Although modifying YSK NPs with a high amount of R8 clearly enhanced the transfection activity (Figure 1), the produced NPs were positively charged (Table 1). This deprives the YSK NPs of its main advantage, namely its non-positive nature under physiological pH. When small densities of R8 are used, the produced NPs were not positively charged, but transfection activities were lower than the corresponding values for the positively charged NPs. It therefore became necessary to enhance the activities of the non-positive YSK-R8 NPs. We have previously shown that multi-layered NPs were superior to single layer NPs in transfecting dividing and non-dividing cells [35,36]. Here, we hypothesized that the transfection activities of YSK/R8-L NPs could be enhanced by preparing double-coated NPs where the R8 peptide is located mainly on the surface of the inner coat and the outer coat is mainly composed of YSK (Figure 2A). We speculate that this design allows pDNA to be condensed in the inner lipid while YSK is free and can exert its main function, i.e., enhancing endosomal escape. In addition, the outer lipid layer would be expected to be consumed during endosomal escape thus releasing the pDNA condensed in the R8-modified inner coat. The inner coat can protect pDNA from degradation in the cytosol and the R8 on its surface would be expected to enhance the migration of the nanoparticles to the nucleus [29]. Taken together, the transfection activities of double-coated YSK/R8 NPs would be predicted to be higher than NPs prepared with a single coating step.

To test this hypothesis, we optimized the amount of R8 in the inner coat to finally produce negatively charged NPs that can be further coated with the positively charged YSK outer lipid (Figure 2B). The water bath sonication used in preparing the inner coat did not significantly affect the integrity of pDNA, especially when the amount of R8 was higher than 4 mol% of lipid, as judged by gel electrophoresis (Supplementary Figure S1A). We have previously shown that pDNA complexed with the polycation poly-l-lysine was not affected by water bath sonication [32]. The second coating significantly improved the EE of pDNA and dramatically increased transfection activities (Figure 2D-E). The transfection activities of 2-step coated NPs were comparable to the efficient commercially available LF reagent (Supplementary Figure S2). Although the transfection is enhanced by increasing the amount of R8 in inner coat, the EE decreased and the surface charge was sometimes positive. To avoid the presence of a positive charge and to obtain a higher EE, we chose NPs prepared with R8 4.5 mol% of inner lipids for further optimization. To estimate the possibility of the formation of NPs coated only with the second coat, we measured the pDNA that remained free after first coat using a sensitive picogreen assay (Supplementary Figure S1B). The free DNA decreased as the percent of R8 increased and the second coat further decreased the free DNA, especially when R8 is low (4 mol%). From this figure, we estimate the amount of DNA coated with the second coat only as 20% (R8-4 mol%), 7% (R8-5 mol%) and 1% (R8-6 mol%). The final optimized NPs contain 4.5 mol% of R8 and the total lipid amount is increased from 320 to 640 nmol which slightly affected the percent of free DNA (Supplementary Figure S1C). We estimate the amount of DNA coated with the second coat only as 14% (320 nmol lipid) and 12% (640 nmol lipid). In addition, the activity of pDNA coated with YSK/Chol (second coat) only is relatively low (Figure 5).

Therefore, we expect that the overall activity may be slightly reduced by the possible presence of single-coated NPs. This does not affect the high transfection activities of optimized YSK/R8-L.

After optimization of the total amount of lipid, as shown in Figure 3, we directly compared the transfection activities of YSK/R8 NPs prepared with the same lipid composition but using the one-step or two-step coating protocols (Figure 4A). When using low amounts of R8, the two-step coated NPs produced much higher transfection activities compared to the one-step coated NPs. Meanwhile, there was no difference in transfection activities between one-step and two-step coating in the case of a high amount of R8.When using a high amount of R8, the peptide is located in the outer layer in both designs and the NPs carry a net positive charge. The high amount of R8 may be sufficient to condense and protect pDNA, irrespective of whether they are prepared in one-step or two-step coating designs, and excess R8 is found free (unbound) on the surface. The higher transfection activities of double-coated YSK/R8-L NPs compared to those prepared with 1-step coating was quite interesting and needed further investigation. Although the activities of 2-step coated R8-L and R8-H NPs were comparable, using low R8 amount provides an additional advantage related to the absence of a final net positive charge. Non-positive NPs are expected to be more serum-resistant and be more suited for in vivo applications. Figure 4B confirms that YSK/R8-L is relatively more serum resistant compared to positively charged YSK/R8-H.

The high transfection activities of the double-coated YSK-R8 NPs point out to the possibility of synergism between YSK and R8. The use of YSK alone or R8 alone failed to produce high transfection activities while the combination of YSK and a low R8 density produced much higher activities, especially when the two-step design was used (Figure 5A). DOPE/R8-H showed higher activities compared to YSK NPs but the highest activities were found for

YSK/R8-H (Figure 5B). This result indicates the existence of synergism between YSK and R8 in both negative and positive NPs and confirms the superiority of double-coated NPs when the amount of R8 is low. To examine the mechanism responsible for this synergism, we compared the cellular uptake of different double-coated NPs (Figure 6). Cellular uptake was significantly improved when a combination of YSK and low R8 was used compared to using YSK alone or R8 alone. In contrast, a high amount of R8 caused a high cellular uptake, even in the absence of YSK. High levels of R8 on the outer surface cause the NPs to adopt a positive charge, thus making them readily internalized. The uptake study, however, is not sufficient to explain the synergism obtained when measuring luciferase activity. This is evident by comparing the efficiency of transfection per internalized DNA (Figure 6E). The efficiency was found to be low for YSK NPs lacking R8 and for DOPE/R8 NPs lacking YSK, which indicates that intracellular trafficking is not optimal. The efficiency was significantly higher when a combination of YSK and R8 was used. YSK is known to improve endosomal escape but the role of R8 in improving intracellular trafficking is not currently clear. We hypothesize that R8 may improve the interaction between YSK in NPs and negatively charged endosomal membranes which may improve YSK fusiogenic activity and enhance endosomal escape. Confocal images of co-localization with lysosomes in Figure 7 support this hypothesis. The YSK/R8-L NPs showed a lower colocalization with lysosomes indicating that R8 may augment the activity of YSK regarding endosomal escape. We have previously shown that the R8 peptide significantly improved endosomal escape mediated by GALA, a fusiogenic peptide [27]. Transfection in the presence of the endosome disrupting agent chloroquine confirmed that YSK endosomal escape behavior is different in the absence or the presence of R8 (Figure 8). Another possibility to explain the enhanced endosomal escape in the presence of R8 is related to the involvement of

YSK in condensing pDNA as explained earlier. When YSK is used as an outer lipid, it functions only as an endosomal escape device and may exert maximum activity. In contrast, in the absence of R8 or when using low levels of R8 in the one-step coating design, YSK is involved in pDNA condensation, which may limit its ability to cause efficient endosomal escape. Other than the effect of R8 on endosomal escape, the possibility exists that the pDNA is released from endosomes in the form of an inner coat where it is protected by the DOPE/R8 lipid. This lipid coat protects DNA from degradation in the cytosol and the outer R8 may improve nuclear migration and internalization. Although confocal images in Figure 7 did not clearly confirm pDNA nuclear delivery in the presence or absence of R8, these images were taken after a short 3 hr chase. Nuclear delivery may be evident at later points, especially when the nuclear envelope is removed during cell division. In addition, some pDNA may be delivered to the nucleus in non-condensed diffused form for which fluorescence could not be detected due to resolution limitations. The role of R8 and other CPP peptides in improving nuclear migration and delivery has been previously shown [37–39]. We are currently performing additional investigations to clarify the role of R8 in enhancing the nuclear delivery of pDNA after endosomal escape.

One interesting result is the enhanced cellular uptake of double-coated YSK/R8-L compared to YSK NPs. First, we did not expect that the cellular uptake of double-coated YSK/R8-L might be significantly improved compared to YSK NPs, since the outer layer is composed mainly of YSK with little or no R8 on the surface. However, the cellular uptake of double-coated YSK/R8-L NPs was higher than YSK NPs by ~6 fold (Figure 6B). We hypothesize that the double-coated design may enable YSK to be in a free state, i.e. not bound to pDNA as in the single-coated NPs. Another possibility is that a certain degree of lipid mixing may occur between the inner and the outer lipids, which allows some of R8 to be expressed on the surface. This suggested surface R8

is low, since it did not cause a change in the net surface charge, but sufficient to enhance interactions with cellular membranes. To test this hypothesis, we investigated the cellular uptake of YSK-liposomes (without pDNA) prepared with or without various amounts of R8 compared to YSK-NPs encapsulating pDNA (1-step coating) (Supplementary Figure S3A). We found a significant difference in cellular uptake in the presence or the absence of pDNA when R8 is used in low amount while the presence of pDNA did not affect the cellular uptake when R8 is used in high amount (>7.2 nmol). Surprisingly, a low amount of R8 on the surface (1.8 nmol, or 0.28 mol% of total lipid) caused a significant increase in cellular uptake in the absence of DNA (~6 fold). This increase was not seen in the presence of DNA, which indicates that pDNA probably consumed the R8 completely when found in low amount in the ordinary one-step coating. We also compared the cellular uptake of YSK-liposomes (without pDNA) with YSK-NPs encapsulating pDNA (1-step or 2-step coating) in the absence or the presence of 7.2 nmol R8 (similar to the optimized YSK-R8-L) (Supplementary Figure S3B). In the presence of pDNA, the cellular uptake was higher in the case of 2-step coating compared to 1-step coating. This supports our hypothesis that in the 2-step coated system, the pDNA is bound in the inner coat and a little R8 is expressed on the surface (free from pDNA), probably through lipid mixing. This little R8 significantly improved cellular uptake compared to the 1-step coating as shown earlier. The mean fluorescence of ~600 arbitrary units (shown in 2-step coated system, R8 7.2 nmol) corresponds to ~1.8 nmol external R8. Therefore, we estimate that ~25% of the R8 in the inner coat may be expressed at the surface and significantly affects cellular uptake. In the case of 1-step coating, much lower free R8 is available at the surface and the effect on cellular uptake is low. The same explanation can also be expected for the interaction between the outer lipid layer and endosomal membranes to improve endosomal escape.

5. CONCLUSION

We report herein on the development of an efficient gene delivery system based on synergism between a pH-sensitive cationic lipid (YSK05) and the R8 peptide. Controlling the amount of R8 and using a two-step coating strategy to confine DNA and most of the R8 to the inner coat permitted us to prepare an efficient, non-positively-charged system. The proposed system described in this study has a considerable potential for use in gene transfer in vivo since it shows improved serum resistance compared to cationic systems that are commonly used for non-viral gene delivery. In addition, the surface of the outer coat can be further modified with different ligands for successful active targeting to different organs.

Conflict of interest

The authors declare no competing financial interest.

ACKNOWLEDGMENT

This work was supported by the Special Education and Research Expenses from the Ministry of Education, Culture, Sports, Science and Technology (MEXT) - Japan. We are grateful for Dr. Abu-Baker M. Abdel-Aal for his helpful comments. We thank Wataru Mizumura and Shoshiro Yamamoto for their technical assistance. We also thank Dr. Milton Feather for his helpful advice in writing this manuscript.

REFERENCES

[1] A. Mountain, Gene therapy: The first decade, Trends Biotechnol. 18 (2000) 119–128. doi:10.1016/S0167-7799(99)01416-X.

[2] K.B. Kaufmann, H. Büning, A. Galy, A. Schambach, M. Grez, Gene therapy on the move, EMBO Mol. Med. 5 (2013) 1642–1661. doi:10.1002/emmm.201202287.

[3] M. Collins, A. Thrasher, Gene therapy: progress and predictions, Proc R Soc B. 282 (2015) 20143003. doi:10.1098/rspb.2014.3003.

[4] A.N. Lukashev, A.A. Zamyatnin, Viral Vectors for Gene Therapy: Current State and Clinical Perspectives., Biochem. Biokhimiia. 81 (2016) 700–8. doi:10.1134/S0006297916070063.

[5] L. Vannucci, M. Lai, F. Chiuppesi, L. Ceccherini-Nelli, M. Pistello, Viral vectors: a look back and ahead on gene transfer technology., New Microbiol. 36 (2013) 1–22. http://www.ncbi.nlm.nih.gov/pubmed/23435812.

[6] F. Liu, L. Huang, Development of non-viral vectors for systemic gene delivery, J. Control. Release. 78 (2002) 259–266. doi:10.1016/S0168-3659(01)00494-1.

[7] H. Yin, R.L. Kanasty, A.A. Eltoukhy, A.J. Vegas, J.R. Dorkin, D.G. Anderson, Non-viral vectors for gene-based therapy, Nat. Rev. Genet. 15 (2014) 541–555. doi:10.1038/nrg3763.

[8] V.P. Torchilin, T. Levchenko, R. Rammohan, N. Volodina, B. Papahadjopoulos-Sternberg, G. D'Souza, Cell transfection in vitro and in vivo with nontoxic TAT peptide-liposome-DNA complexes, Proc Natl Acad Sci U S A. 100 (2003) 1972–1977. doi:10.1073/pnas.0435906100 [pii].

[9] K. Itaka, K. Kataoka, Recent development of nonviral gene delivery systems with virus-like structures and mechanisms, Eur. J. Pharm. Biopharm. 71 (2009) 475–483. doi:10.1016/j.ejpb.2008.09.019.

[10] A. Delalande, M. Gosselin, A. Suwalski, W. Guilmain, C. Leduc, M. Berchel, P. Jaffrès, P. Baril, P. Midoux, C. Pichon, Enhanced Achilles tendon healing by fibromodulin gene transfer, Nanomedicine Nanotechnology, Biol. Med. 11 (2015) 1735–1744. doi:10.1016/j.nano.2015.05.004.

[11] M.F. Lindberg, T. Gall, N. Carmoy, M. Berchel, S.C. Hyde, D.R. Gill, P. Jaffres, P. Lehn, T. Montier, Efficient in vivo transfection and safety profi le of a CpG-free and codon optimized luciferase plasmid using a cationic lipophosphoramidate in a multiple intravenous administration procedure, Biomaterials. 59 (2015) 1–11. doi:10.1016/j.biomaterials.2015.04.024.

[12] M. Foldvari, D.W. Chen, D. Calderon, L. Narsineni, A. Rafiee, Non-viral gene therapy : Gains and challenges of non-invasive administration methods, J. Control. Release. 240 (2016) 165–190. doi:10.1016/j.jconrel.2015.12.012.

[13] V.K. Yellepeddi, Vectors for Non-viral Gene Delivery - Clinical and Biomedical

Applications, Austin Ther. 2 (2015) 1–8.

[14] M. Rogers, R.A. Rush, Non-viral gene therapy for neurological diseases , with an emphasis on targeted gene delivery, J. Control. Release. 157 (2012) 183–189. doi:10.1016/j.jconrel.2011.08.026.

[15] F. Perche, D. Gosset, M. Mével, M.-L. Miramon, J.-J. Yaouanc, C. Pichon, T. Benvegnu, P.-A. Jaffrès, P. Midoux, Selective gene delivery in dendritic cells with mannosylated and histidylated lipopolyplexes, J. Drug Target. 19 (2011). doi:10.3109/1061186X.2010.504262.

[16] E.W.F.W. Alton, D.K. Armstrong, D. Ashby, K.J. Bayfi, D. Bilton, E. V Bloomfi, A.C. Boyd, J. Brand, R. Buchan, R. Calcedo, P. Carvelli, M. Chan, S.H. Cheng, D.D.S. Collie, S. Cunningham, H.E. Davidson, G. Davies, J.C. Davies, L.A. Davies, M.H. Dewar, A. Doherty, J. Donovan, N.S. Dwyer, H.I. Elgmati, R.F. Featherstone, J. Gavino, S. Gea-sorli, D.M. Geddes, J.S.R. Gibson, D.R. Gill, A.P. Greening, U. Griesenbach, D.M. Hansell, K. Harman, T.E. Higgins, S.L. Hodges, S.C. Hyde, L. Hyndman, J.A. Innes, J. Jacob, N. Jones, B.F. Keogh, M.P. Limberis, P. Lloyd-evans, A.W. Maclean, M.C. Manvell, G.D. Murray, A.G. Nicholson, T. Osadolor, J. Parra-leiton, D.J. Porteous, I.A. Pringle, E.K. Punch, K.M. Pytel, A.L. Quittner, G. Rivellini, C.J. Saunders, R.K. Scheule, S. Sheard, N.J. Simmonds, K. Smith, S.N. Smith, N. Soussi, S. Soussi, E.J. Spearing, B.J. Stevenson, S.G. Sumner-jones, M. Turkkila, R.P. Ureta, M.D. Waller, Repeated nebulisation of non-viral CFTR gene therapy in patients with cystic fibrosis : a randomised , double-blind , placebo-controlled , phase 2b trial, Lancet Respir Med. 3 (2015) 684–91. doi:10.1016/S2213-2600(15)00245-3.

[17] T. Lehto, K. Ezzat, M.J.A. Wood, S. EL Andaloussi, Peptides for nucleic acid delivery, Adv. Drug Deliv. Rev. 106 (2016) 172–182. doi:10.1016/j.addr.2016.06.008.

[18] A. Aied, U. Greiser, A. Pandit, W. Wang, Polymer gene delivery: Overcoming the obstacles, Drug Discov. Today. 18 (2013) 1090–1098. doi:10.1016/j.drudis.2013.06.014.

[19] X.X. Zhang, T.J. McIntosh, M.W. Grinstaff, Functional lipids and lipoplexes for improved gene delivery, Biochimie. 94 (2012) 42–58. doi:10.1016/j.biochi.2011.05.005.

[20] Y. Sato, H. Hatakeyama, Y. Sakurai, M. Hyodo, H. Akita, H. Harashima, A pH-sensitive cationic lipid facilitates the delivery of liposomal siRNA and gene silencing activity in vitro and in vivo, J. Control. Release. 163 (2012) 267–276. doi:10.1016/j.jconrel.2012.09.009.

[21] Y. Sato, H. Hatakeyama, M. Hyodo, H. Harashima, Relationship between the Physicochemical Properties of Lipid Nanoparticles and the Quality of siRNA Delivery to Liver Cells., Mol. Ther. 24 (2015) 788–795. doi:10.1038/mt.2015.222.

[22] Y. Sato, T. Nakamura, Y. Yamada, H. Harashima, Development of a multifunctional envelope-type nano device and its application to nanomedicine, J. Control. Release. 244 (2016) 194–204. doi:10.1016/j.jconrel.2016.06.042.

[23] H. Hatakeyama, M. Murata, Y. Sato, M. Takahashi, N. Minakawa, A. Matsuda, H.

Harashima, The systemic administration of an anti-miRNA oligonucleotide encapsulated pH-sensitive liposome results in reduced level of hepatic microRNA-122 in mice, J. Control. Release. 173 (2014) 43–50. doi:10.1016/j.jconrel.2013.10.023.

[24] T. Watanabe, H. Hatakeyama, C. Matsuda-Yasui, Y. Sato, M. Sudoh, A. Takagi, Y. Hirata, T. Ohtsuki, M. Arai, K. Inoue, H. Harashima, M. Kohara, In vivo therapeutic potential of Dicer-hunting siRNAs targeting infectious hepatitis C virus., Sci. Rep. 4 (2014) 4750. doi:10.1038/srep04750.

[25] Y. Sakurai, T. Matsuda, T. Hada, H. Harashima, Efficient Packaging of Plasmid DNA Using a pH Sensitive Cationic Lipid for Delivery to Hepatocytes, Biol. Pharm. Bull. 38 (2015) 1185–1191. doi:10.1248/bpb.b15-00138.

[26] I.A. Khalil, K. Kogure, S. Futaki, S. Hama, H. Akita, M. Ueno, H. Kishida, M. Kudoh, Y. Mishina, K. Kataoka, M. Yamada, H. Harashima, Octaarginine-modified multifunctional envelope-type nanoparticles for gene delivery, Gene Ther. 14 (2007) 682–689. doi:10.1038/sj.gt.3302910.

[27] I.A. Khalil, Y. Hayashi, R. Mizuno, H. Harashima, Octaarginine- and pH sensitive fusogenic peptide-modified nanoparticles for liver gene delivery, J. Control. Release. 156 (2011) 374–380. doi:10.1016/j.jconrel.2011.08.012.

[28] Y. Hayashi, R. Mizuno, I.A. Khalil, H. Akita, H. Harashima, Pretreatment of hepatocyte growth factor gene transfer mediated by octaarginine peptide-modified nanoparticles ameliorates LPS/D-galactosamine-induced hepatitis, Nucleic Acid Ther. 22 (2012) 360–3. doi:10.1089/nat.2012.0352.

[29] I.A. Khalil, K. Kogure, S. Futaki, H. Harashima, Octaarginine-modified liposomes: Enhanced cellular uptake and controlled intracellular trafficking, Int. J. Pharm. 354 (2008) 39–48. doi:10.1016/j.ijpharm.2007.12.003.

[30] I.A. Khalil, K. Kogure, S. Futaki, H. Harashima, High density of octaarginine stimulates macropinocytosis leading to efficient intracellular trafficking for gene expression, J. Biol. Chem. 281 (2006) 3544–3551. doi:10.1074/jbc.M503202200.

[31] Y. Hayashi, J. Yamauchi, I.A. Khalil, K. Kajimoto, H. Akita, H. Harashima, Cell penetrating peptide-mediated systemic siRNA delivery to the liver, Int. J. Pharm. 419 (2011) 308–313. doi:10.1016/j.ijpharm.2011.07.038.

[32] K. Kogure, R. Moriguchi, K. Sasaki, M. Ueno, S. Futaki, H. Harashima, Development of a non-viral multifunctional envelope-type nano device by a novel lipid film hydration method, J. Control. Release. 98 (2004) 317–323. doi:10.1016/j.jconrel.2004.04.024.

[33] L.D. Cervia, C.C. Chang, L. Wang, F. Yuan, Distinct effects of endosomal escape and inhibition of endosomal trafficking on gene delivery via electrotransfection, PLoS One. 12 (2017) 1–18. doi:10.1371/journal.pone.0171699.

[34] M. Tamaru, H. Akita, T. Nakatani, K. Kajimoto, Y. Sato, H. Hatakeyama, H. Harashima, Application of apolipoprotein E-modified liposomal nanoparticles as a carrier for

delivering DNa and nucleic acid in the brain, Int. J. Nanomedicine. 9 (2014) 4267–4276. doi:10.2147/IJN.S65402.

[35] S.M. Shaheen, H. Akita, T. Nakamura, S. Takayama, S. Futaki, A. Yamashita, R. Katoono, N. Yui, H. Harashima, KALA-modified multi-layered nanoparticles as gene carriers for MHC class-I mediated antigen presentation for a DNA vaccine, Biomaterials. 32 (2011) 6342–6350. doi:10.1016/j.biomaterials.2011.05.014.

[36] H. Akita, A. Kudo, A. Minoura, M. Yamaguti, I.A. Khalil, R. Moriguchi, T. Masuda, R. Danev, K. Nagayama, K. Kogure, H. Harashima, Multi-layered nanoparticles for penetrating the endosome and nuclear membrane via a step-wise membrane fusion process, Biomaterials. 30 (2009) 2940–2949. doi:10.1016/j.biomaterials.2009.02.009.

[37] Y. Hu, H. Matthew T., Y. Wang, F. Liu, L. Huang, A highly efficient synthetic vector: nonhydrodynamic delivery of DNA to hepatocyte nuclei in vivo, ACS Nano. 7 (2013) 5376–5384. doi:10.1021/nn4012384.

[38] B. Gupta, T.S. Levchenko, V.P. Torchilin, Intracellular delivery of large molecules and small particles by cell-penetrating proteins and peptides, Adv. Drug Deliv. Rev. 57 (2005) 637–651. doi:10.1016/j.addr.2004.10.007.

[39] S.B. Fonseca, M.P. Pereira, S.O. Kelley, Recent advances in the use of cell-penetrating peptides for medical and biological applications, Adv. Drug Deliv. Rev. 61 (2009) 953–964. doi:10.1016/j.addr.2009.06.001.

FIGURE LEGENDS

Figure 1. Comparison of transfection activities of luciferase-encoding plasmid DNA encapsulated in different YSK NPs

Cells were transfected with YSK NPs in the absence (YSK) or the presence of low or high amount of R8 (YSK/R8-L or YSK/R8-H, respectively). Luciferase activity was measured after 24 hr and is expressed as relative light units per mg of total proteins (RLU/mg protein). Each bar represents the mean +/- SD of 3 different experiments (*P<0.05, **P<0.001 vs. YSK).

Figure 2. Preparation and evaluation of double-coated YSK/R8 NPs

A. Schematic illustration of the preparation of double-coated YSK/R8-L NPs. The pDNA was first coated with a lipid layer consisting of DOPE/STR-R8 to form NPs with a net negative charge. These NPs were then coated with a YSK05/cholesterol layer under acidic conditions. B. Surface charges of NPs prepared by coating pDNA with DOPE and varying amounts of STR-R8 (mean +/- SEM of at least 4 different preparations). C. Characterization of NPs prepared with different R8 amounts after second coating (mean +/- SEM of 4 different preparations). D. Encapsulation efficiency (EE) of pDNA after first or second coat (mean +/- SD of 3 different preparations). E. Transfection activities of different NPs prepared with one- or two-step coating. Each bar represents the mean +/- SD of 3 different experiments (*P<0.05, **P<0.01 vs. [After 1st coat]).

Figure 3. Optimization of double-coated YSK/R8-L NPs

A. Characterization of different YSK/R8-L NPs prepared using different amounts of lipids (mean +/- SD of at least 3 different preparations). B. Encapsulation efficiency (EE) of YSK/R8-L NPs prepared using different lipid amounts (mean +/- SD of at least 3 different preparations) (*P<0.05, **P<0.01 vs. original condition (320 nmol lipid)). C. Transfection activities of double-coated YSK/R8-L NPs prepared using different amounts of lipid. Each bar represents the mean +/- SD of 3 different experiments.

Figure 4. Comparison of transfection activities of different NPs prepared with 1-step or 2-step coating

A. Cells were transfected with YSK/R8-L or YSK/R8-H NPs prepared using 1-step or 2-step coating. Luciferase activity is expressed as relative light unit per mg of total proteins (RLU/mg protein). Each bar represents the mean +/- SD of 3 different experiments (*P<0.05 vs. 1-step coating). B. Transfection activities in the presence of 10% serum (expressed as % of luciferase activities in the absence of serum). Each bar represents the mean +/- SD of 3 different experiments (*P<0.05 vs. YSK/R8-H).

Figure 5. Synergism between YSK05 and R8

Cells were transfected with different NPs prepared with YSK05/DOPE in the absence of R8 (YSK) or with DOPE/R8 in the absence of YSK (DOPE/R8-L or -H) or with both YSK05 and R8 (YSK/R8-L or -H). NPs were prepared using 1-step or 2-step coating. A. Low amount of R8 (R8-L). B. High amount of R8 (R8-H). Luciferase activity is expressed as relative light units per

mg of total protein (RLU/mg protein). Each bar represents the mean +/- SD of 3 different experiments (**P<0.01).

Figure 6. Comparison of cellular uptake and transfection efficiency of different NPs

A, C. Histograms showing fluorescence intensities of cells after treatment with different NPs. B, D. Comparison of geo-mean fluorescence in each case. Each bar represents the mean +/- SD of 3 different experiments (*P<0.05, **P<0.01). E. Calculation of efficiency of transfection obtained by dividing luciferase activities from Figure 5 (RLU/mg protein) by cellular uptake (geo-mean fluorescence).

Figure 7. Evaluation of the endosomal escape of different NPs

Confocal laser scanning images of cells treated with NPs encapsulating Cy-5 pDNA (red) followed by staining lysosomes with LysoTracker (green). Cells were treated with naked pDNA, YSK or YSK/R8-L NPs for 1 hr followed by a 3-hr chase period.

Figure 8. Effect of chloroquine on transfection activities of different NPs

Cells were transfected with YSK or YSK/R8-L NPs in the presence or absence of chloroquine. Luciferase activity is expressed as fold increase compared to the absence of chloroquine. Each bar represents the mean +/- SD of at least 3 different experiments (*P<0.05 vs. no-chloroquine condition).

Figures

Figure 1

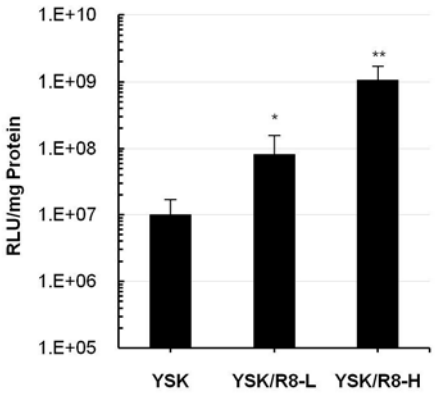

Figure 2

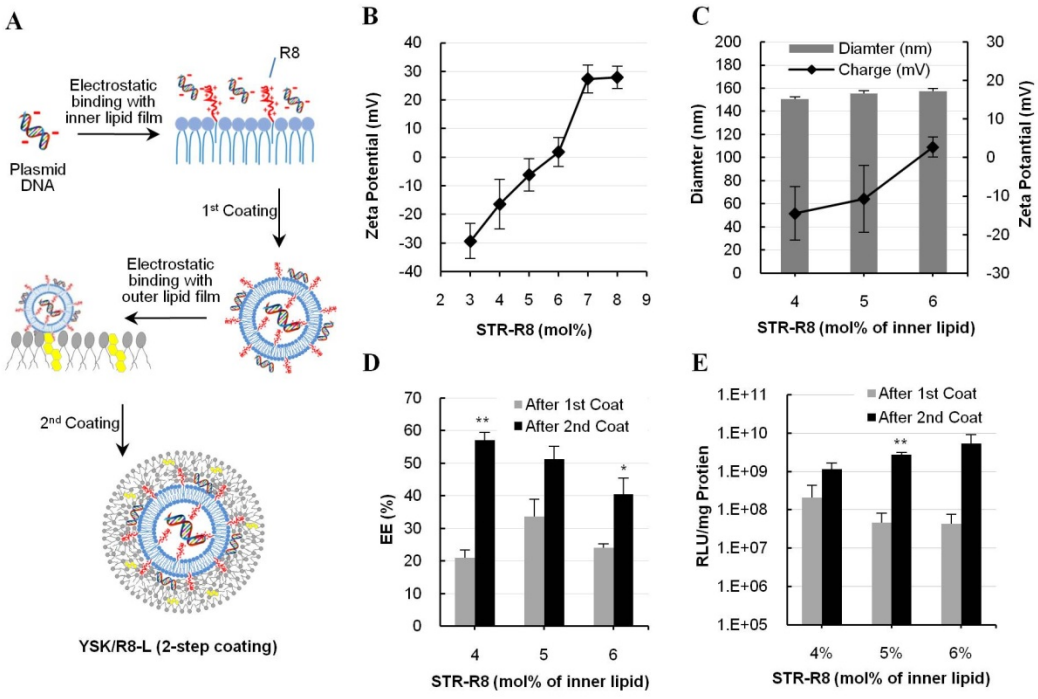

Figure 3

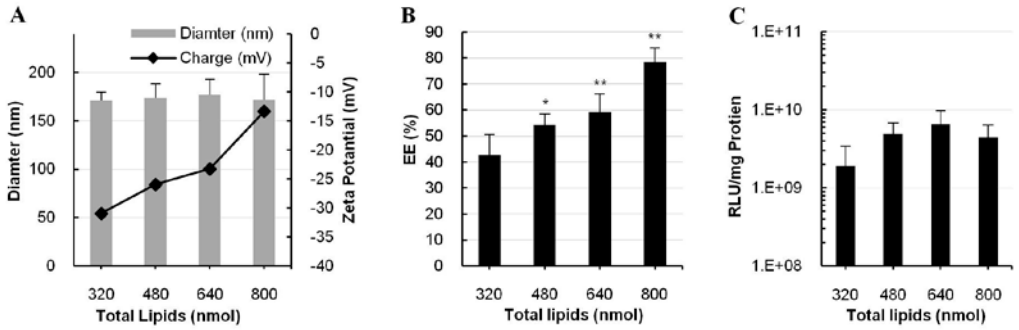

Figure 4

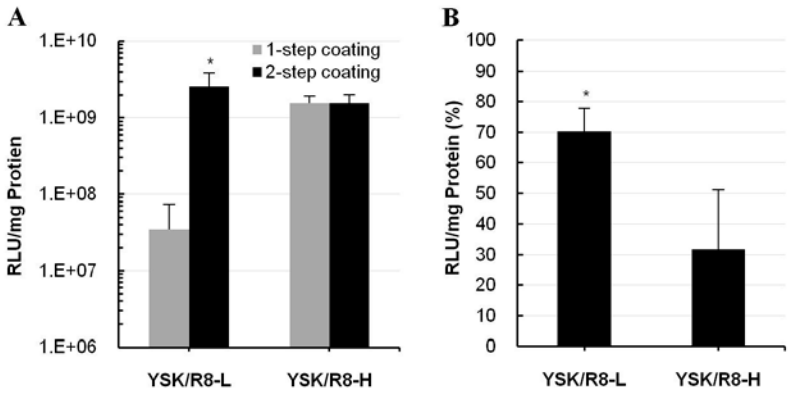

Figure 5

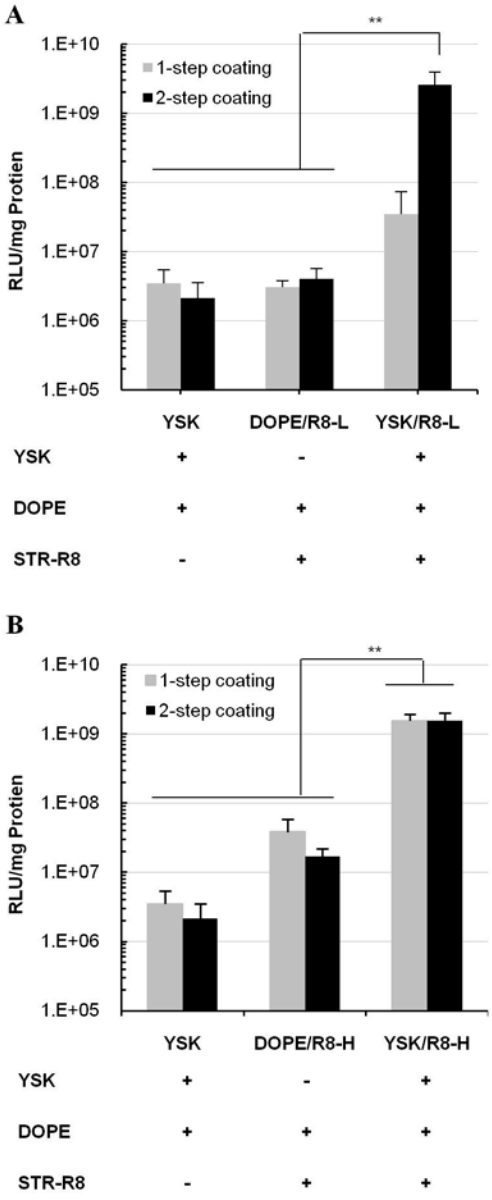
A
**
1.E+10
1.E+09
1.E+08
1.E+07
1.E+06
1.E+05
RLU/mg Protien
1-step coating
2-step coating
YSK
DOPE/R8-L
YSK/R8-L
YSK + - +
DOPE + + +
STR-R8 - + +
B
**
1.E+10
1.E+09
1.E+08
1.E+07
1.E+06
1.E+05
RLU/mg Protien
1-step coating
2-step coating
YSK
DOPE/R8-H
YSK/R8-H
YSK + - +
DOPE + + +
STR-R8 - + +

Figure 6

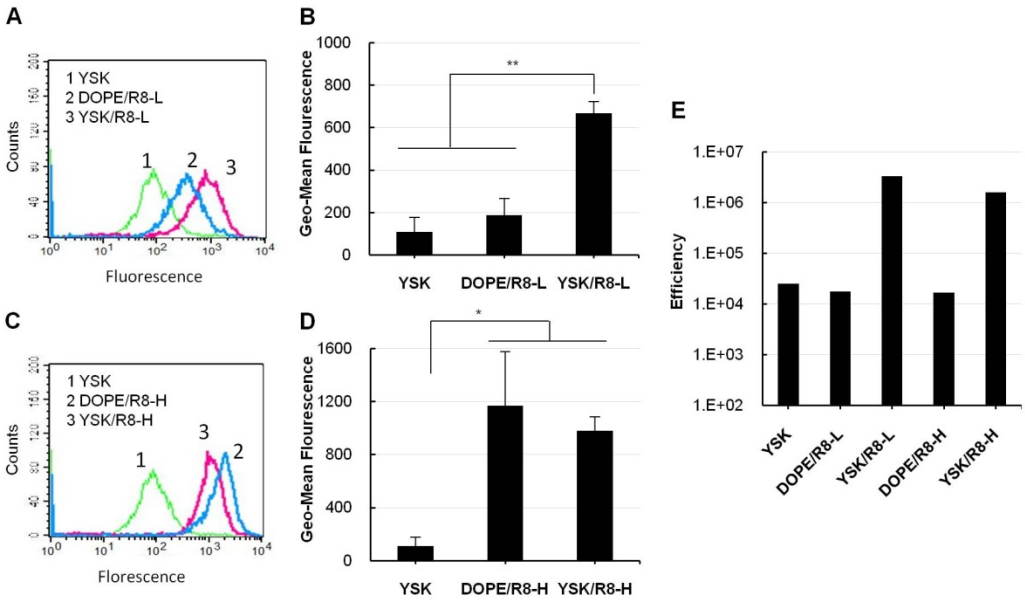

Figure 7

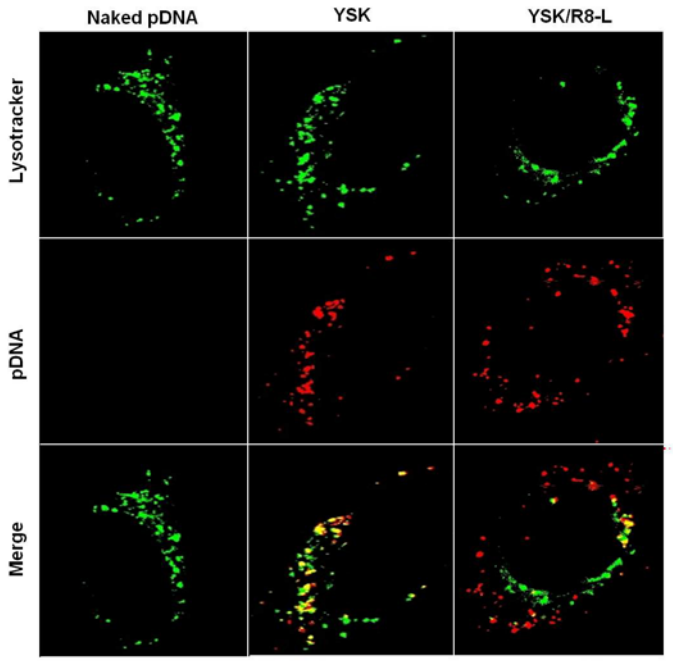

Figure 8

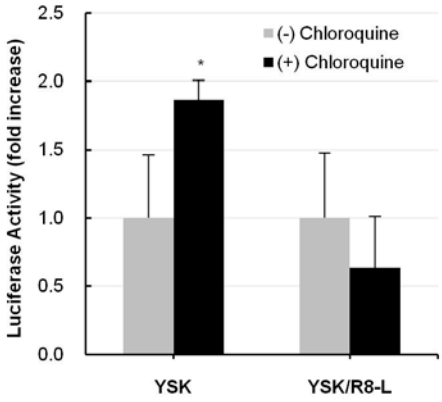
2.5
2.0
1.5
1.0
0.5
0.0
Luciferase Activity (fold increase)
(-) Chloroquine
(+) Chloroquine
*
YSK
YSK/R8-L

Tables

Table 1

TABLE 1. Characterization of YSK nanoparticles*

	STR-R8 content (mol% of total lipids)	Diameter (nm)	PDI	Zeta Potential (mV)
YSK	0	181.5 ± 11.7	0.38 ± 0.06	(-) 20.2 ± 6.8
YSK/R8-L	2	181.4 ± 10.7	0.31 ± 0.06	(-) 19.5 ± 5.8
YSK/R8-H	10	178.1 ± 6.3	0.35 ± 0.13	(+) 22.5 ± 7.5

*Values are the mean +/- SD of at least 3 independent preparations

Table 2

TABLE 2.
Composition and characterization of different nanoparticles prepared by 1-step or 2-step coating*

		Lipid Composition	Diameter (nm)	PDI	Zeta Potential (mV)
YSK/R8-L	1-step coating	YSK:DOPE:Chol:PEG:R8[1] (4:5:1:0.075:0.1125)	168 ± 1	0.270 ± 0.00	(-) 24 ± 7
	2-step coating	*First Coat*- DOPE:R8 (9.775:0.225) *Second Coat*- YSK:Chol:PEG (8:2:0.15)	162 ± 3	0.282 ± 0.02	(-) 27 ± 2
YSK/R8-H	1-step coating	YSK:DOPE:Chol:PEG:R8 (4:5:1:0.075:0.6125)	140 ± 4	0.242 ± 0.07	(+) 34 ± 7
	2-step coating	*First Coat*- DOPE:R8 (9.775:0.225) *Second Coat*- YSK:Chol:PEG:R8 (8:2:0.15:1)	144 ± 1	0.265 ± 0.02	(+) 25 ± 7

*Values are the mean +/- SD of at least 3 different preparations
[1]PEG is used as DMG-PEG-2000 and R8 is used as STR-R8

Graphical Abstract

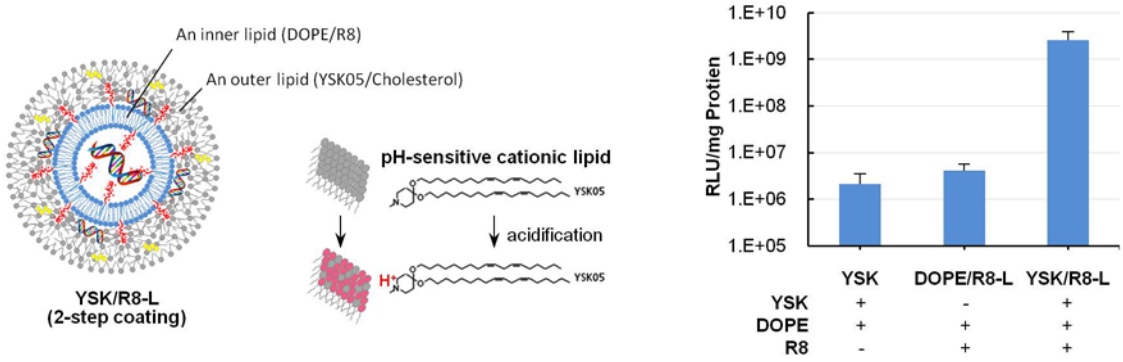

Supplementary Figures

Supplementary Figure S1

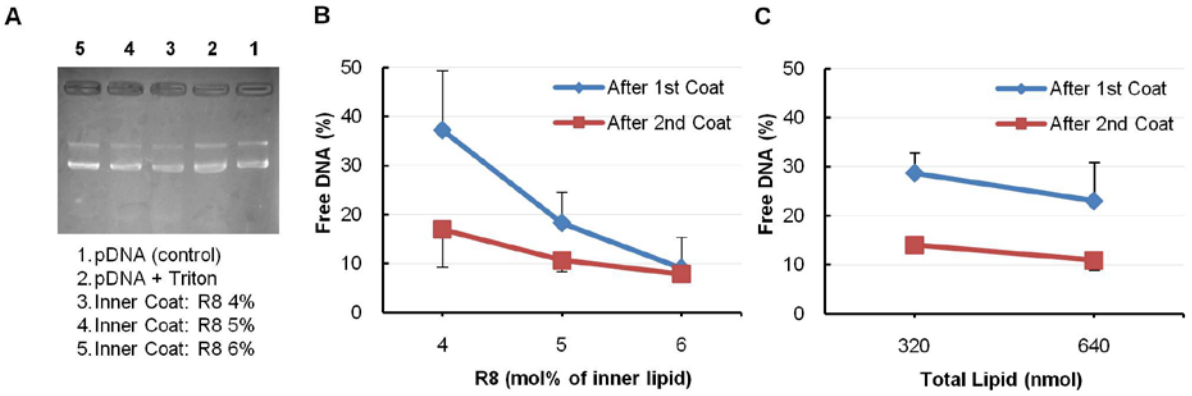

A. Gel electrophoresis of pDNA after lipid coating. Samples of lipid coated NPs containing 0.4 µg DNA were treated with Triton X-100 (final concentration 1%) and dextran (final concentration 1 mg/mL) for 15 min at room temperature before gel electrophoresis. Electrophoresis was performed on 1% agarose gel at 100 V for 30 min and the gel was then stained with ethidium bromide. Naked plasmid DNA (pDNA) was used as a control (+/- Triton). B. Evaluation of free pDNA after first or second lipid coating in the presence of different amounts of R8. Samples were treated with picogreen reagent in the presence (total DNA) or the absence (free DNA) of Triton X-100 and dextran. C. Effect of total lipid amount on the percent free DNA after first or second lipid coating.

Supplementary Figure S2

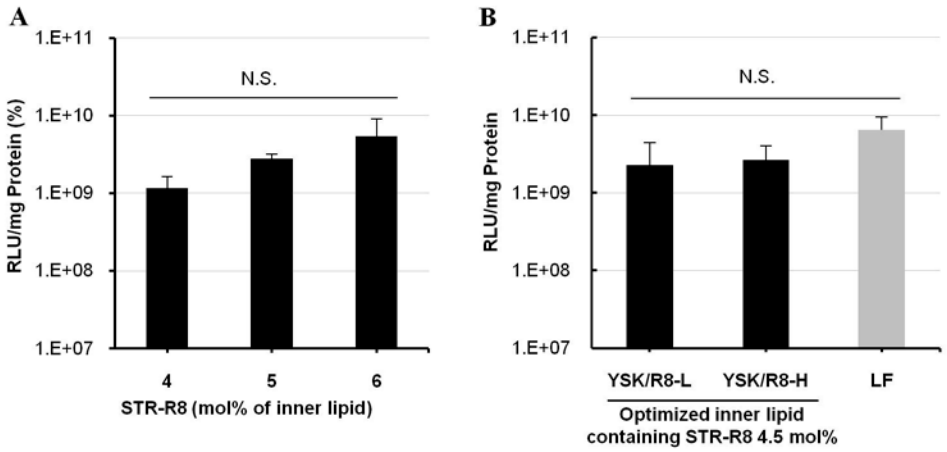

A. Transfection activities of different double-coated YSK/R8-L NPs containing different amounts of R8 in the inner coat (from Figure 2E). B. Direct comparison of transfection activities of YSK/R8 NPs and Lipofectamine 2000 Reagent (LF). YSK/R8 NPs were prepared with the optimized inner coat (STR-R8 4.5 mol% of inner lipid). Luciferase activities were measured after 24 hr and expressed as relative light units per mg of total proteins (RLU/mg protein). Each bar represents the mean +/- SD of at least 3 different experiments (N.S. is no statistical significant difference).

Supplementary Figure S3

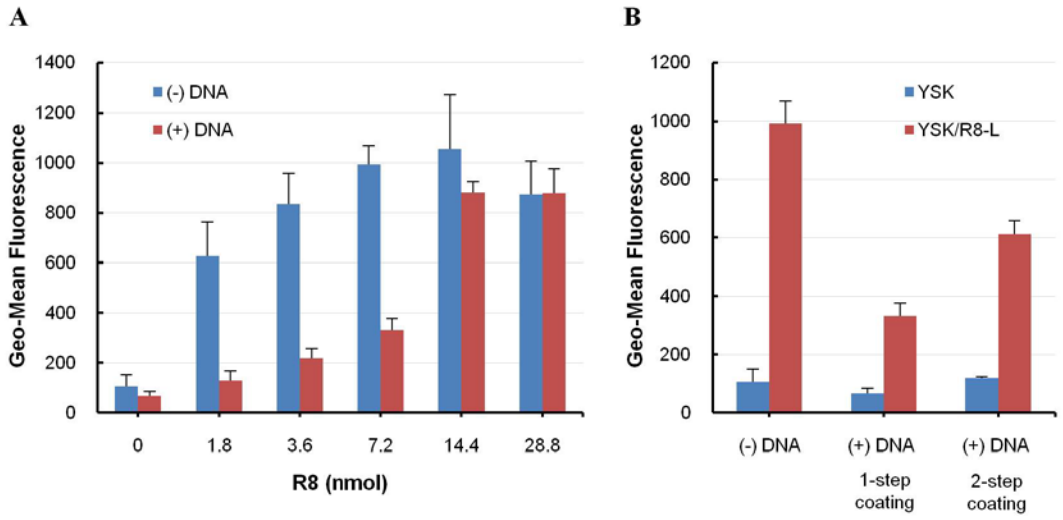

A. Cellular uptake of YSK-liposomes (prepared in the absence of pDNA) and YSK-NPs (prepared with pDNA, 1-step coating) in the presence of variable amounts of R8. B. Direct comparison of cellular uptake of YSK-liposomes and YSK-NPs (1-step or 2-step) coating prepared in the absence or the presence of R8 (7.2 nmol, optimized condition). Cellular uptake is expressed as geo-mean fluorescence measured in each case. Each bar represents the mean +/- SEM of 3 different experiments.